Ionics (2012) 18:413–423
DOI 10.1007/s11581-011-0636-1

ORIGINAL PAPER

# A dielectric relaxation study of starch–water and starch–glycerol films

**Perumal Ramasamy**

Received: 7 December 2010 / Revised: 11 September 2011 / Accepted: 6 October 2011 / Published online: 26 October 2011


**Keywords** Batteries · Li conductors · Lithium batteries · Polymer electrolytes · Relaxations

## Introduction

The use of starch as a solid polymer electrolyte (SPE) has gained interest recently due to its desirable qualities that include biodegradability, low production cost, and good physical and chemical properties [1, 2]. Starch is a natural polymer that is present in plants in the form of granules. It is found in the form of granules that vary in size (1–100 μm). Starch consists of amylose and amylopectin. Amylose is a linear or lightly branched (1→4)-linked α-glucan of MW $10^5$–$10^6$ while amylopectin is a highly branched molecule of MW $10^7$–$10^9$ containing numerous (1→4)-linked α-glucan chains linked (1→6) [3]. Linear polymers typically crystallize more readily than branched polymers [4]. As starch consists of both amylose and amylopectin, with only amylose contributing to the crystallinity, it becomes very essential to understand the mechanisms that govern the dynamics of the polymer molecules along with the role of plasticizers that contain charged groups. Additionally, the presence of networks in the films can contribute significantly to important physical properties like electrical conductivity. Dielectric relaxation spectroscopy (DRS) has been found to be a very useful tool in studying the polymer dynamics of polysaccharides [5, 6]. Dielectric spectroscopy can help us understand better the dynamics of the molecules and the mechanisms that occur at the interphase of crystalline and amorphous regions which cannot be explored by other techniques. Dielectric relaxation spectroscopy is a useful way to study the changes in the molecular dynamics of polysaccharides influenced by its interactions with water [7–11]. The dielectric characteristics of starch have been shown to be highly influenced by the presence of water [12, 13]. Butler et al. have identified different relaxations in starch by studying solid starch and dextran [13]. They have shown that at low temperatures (from −120 to −90 °C), a relaxation ($\gamma_1$) obeying Arrhenius behavior is observed and it was attributed to motions of small parts of amylose, amylopectin, and dextran. The typical activation energies lay from 50 to 65 kJ $mol^{-1}$. At temperatures lower than that, another relaxation ($\gamma_2$) exists and was observed only in dry starch [13]. Its presence was attributed to the rotation of methylol group present on the amylose and amylopectin molecules in starch. At temperatures between 0 and 50 °C, another local relaxation ($\beta$) was shown to exist that was highly dependent upon water content. Its presence was attributed to the increase in the mobility of large segments of amylose and amylopectin molecules. Further, Butler et al. have shown the presence of another relaxation ($\alpha$) between 60 and 80 °C in granular starch and was attributed to the increase of mobility of amylose and amylopectin molecules upon swelling of and release of starch molecules during gelatinization. Starch films made from using water are usually very brittle. Glycerol is one commonly employed plasticizer [14–18]. Addition of glycerol as a plasticizer greatly reduces the $T_g$ of the films, making it

**Electronic supplementary material** The online version of this article (doi:10.1007/s11581-011-0636-1) contains supplementary material, which is available to authorized users.

P. Ramasamy (✉)
Department of Physics, Anna University,
Chennai, India
e-mail: perumalramasamy@annauniv.edu

convenient for studying the dielectric relaxation properties. Studies relating to amylose–glycerol systems and amylose–glycerol–water systems have suggested that glycerol and starch are partially miscible [18, 19]. The aim of the study is to observe changes in the dielectric behavior of starch as a function of water and glycerol content. The conductivities of starch with glycerol systems to which 5 wt.% $LiClO_4$ salt was added were also investigated.

## Experimental procedure

### Materials and methods

Corn starch (Amioca) was used for our study. It was purchased from National Starch Company. Films obtained by casting only water solutions were found to be very brittle. Hence, two sets of samples were made for (1) starch with varying quantities of water content and (2) starch with varying quantities of glycerol. The procedure for the preparation of the two types of sample is as detailed below:

(1) Starch with varying quantities of water: samples were made in the form of discs by hot pressing starch powder between brass discs of diameter 30 mm at 1,900 bar for 15 min. The thickness of the discs was 0.4–0.5 mm. For making dry samples (0% water), the discs were annealed in a vacuum oven at 100 °C for 24 h. Discs were also placed inside sealed containers having $MgNO_3$ and NaCl salt for at least 2 weeks to achieve a relative humidity of 51% and 75%, respectively.
(2) Starch with varying quantities of glycerol: Here the samples were made in the form of films. Appropriate amounts of glycerol (in weight) were added to starch powder of weight 3 gm to which 100 ml of water was later added and stirred at 90° for 1 h. The solution was then poured into homemade teflon discs and allowed to dry for 24–48 h to get films of starch containing glycerol. The thickness of the films was ~200–250 μm. To study the changes in the conductivities of these glycerol-containing starch films due to addition of $LiClO_4$, 150 mg of LiClO4 was added to 3 gm of starch powder to which an appropriate amount of glycerol had been added. To this mixture, 100 ml of water was later added and stirred at 90° for 1 h. The samples thus obtained had 5 wt.% of $LiClO_4$ in it. The thus obtained starch films were found to be flexible.

In order to minimize the effect of atmospheric water in the DRS measurements, the samples were quickly transferred (less than 10 min) from the sealed containers to the sample holder in the DRS machine.

### Scanning electron microscopy

Scanning electron microscopy (SEM) was done with a FEI QUANTA-200 scanning electron microscope. The samples (starch films) were fixed using carbon tape. The voltage used was 30 kV and the instrument was operated at low vacuum mode.

### XRD

The instrument Bruker D2 phaser was used for obtaining XRD data. The voltage used was 30 kV and 20 mA was used. The counts were measured as a function of $2\theta$. The wavelength used was 1.54184 A.

### Raman measurements

Laser Raman spectrophotometer (Model Aspire 785 L) with a diode laser source of wavelength 785 nm in 150–1,800 $cm^{-1}$ range at room temperature was used for obtaining Raman spectra.

### FTIR measurements

A Perkin Elmer Spectrum One FT-IR spectrometer was used. The spectral resolution was 4 $cm^{-1}$. The sample was placed in between two potassium bromide discs.

### Differential scanning calorimetry

TA Q-100 DSC was used to measure the glass transition temperatures ($T_g$). The sample used was gelatinized starch with 23% glycerol of weight 9.9 mg. The operating temperature was −120 to 150 °C. The sample was in the form of a film. Aluminum pan was used. The sample was cooled from room temperature to −120 °C and allowed to equilibrate at −120 °C for 5 min. It was then ramped up to 150 °C at 10 °C/min. Data were collected as the temperature was increased from −120 to 150 °C.

### Broadband dielectric relaxation spectroscopy

Dielectric relaxation spectra were collected isothermally using a Novocontrol GmBh Concept 40 broadband dielectric spectrometer in the frequency range 0.1–$10^6$ Hz. Temperatures were controlled within 0.2 °C. The samples were prepared by placing the films between well-polished brass discs. The diameter of the top electrode was 15 mm while the diameter of the bottom electrode was 30 mm. The temperature varied from −120 to 100 °C. Starch decomposes at~200 °C. Hence, the experiments were not carried out beyond 150 ° C. In order to measure the dielectric behavior of glycerol, a droplet of glycerol was placed

between brass electrodes separated by using a 50-μm-thick silica spacer. In order to better resolve the spectra due to high values for dielectric loss caused by high conduction loss, the dielectric loss was calculated using the expression [20]:

$$\varepsilon''_{\mathrm{der}} = -(\pi/2)(\partial\varepsilon'(\omega)/\partial \ln\omega) \quad (1)$$

The relaxation positions were determined using WINFIT software.

## Results and discussions

### Morphology of the samples

The optical images and the morphology of the samples of starch films are shown in Fig. 1. It is observed that the starch film containing 23% glycerol (Fig. 1a) is almost transparent and is flexible (Fig. 1b). The starch films containing 23% glycerol and 25% $LiClO_4$ are also transparent and flexible (Fig. 1c, d). Figure 2 shows SEM image for Li $ClO_4$–included starch film (a) and EDAX spectra for Li-doped starch film (b). The inset inside subpanel b shows the elemental composition for carbon, oxygen, and chlorine in the film. The EDAX image shows that the constituents of the film are dispersed in the film. The SEM images for starch films with (1) 0% glycerol (a and b), (2) 23% glycerol (c and d), and (3) 23% glycerol and 5% $LiClO_4$ (e and f) are shown in Fig. 3. From the SEM images it is observed that when there is no glycerol (Fig. 3a, b), there are lots of aggregates and the size of these aggregates ranges from ~1 to 20 μm. The presence of these aggregates is due to the insolubility of starch in water. These aggregates are indicated by the dark circles in the SEM images to aid the eye. For a sample containing 23% glycerol (Fig. 3c, d), it was observed that the films are smooth and the aggregation is much less that those films having no glycerol. However, there are still some small aggregates observed. The sizes of these aggregates are ~1 μm. These tiny aggregates are also observed for starch with 23% glycerol and 5% $LiClO_4$ (Fig. 3e, f). The presence of these tiny aggregates indicates that starch and glycerol are partially miscible.

### XRD, Raman, and FTIR characterizations

*XRD* Figure 4a shows the XRD pattern for starch powder (before formation of film), starch film containing 23% glycerol, and starch film containing 23% glycerol and 5% LiClO4. It is observed that the starch powder is crystalline and shows clear peaks at $2\theta$ values of 14.8, 17.2, 19.6, 22.3, 24.1, 26.4, 30.4, 34.4, and 38.4 and it is of the A form [21]. However, the films do not have well-resolved peaks and their intensities are reduced, indicating an amorphous nature. The decrease in crystallinity is due to the application of heat during the formation of the films.

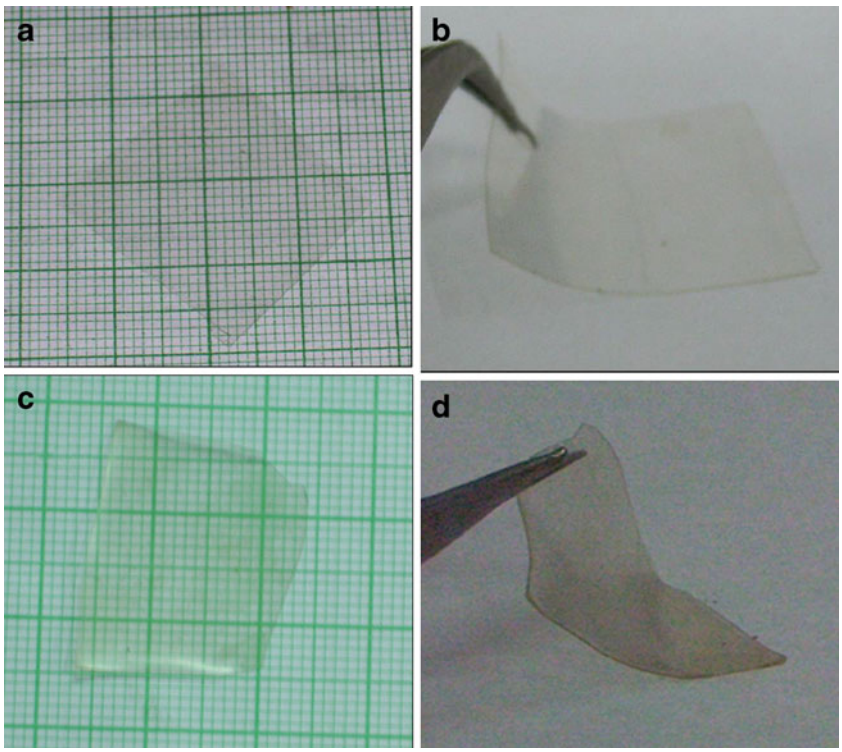


**Fig. 1** **a**, **b** Starch with 23% glycerol. **c**, **d** Starch with 23% glycerol and 5% $LiClO_4$

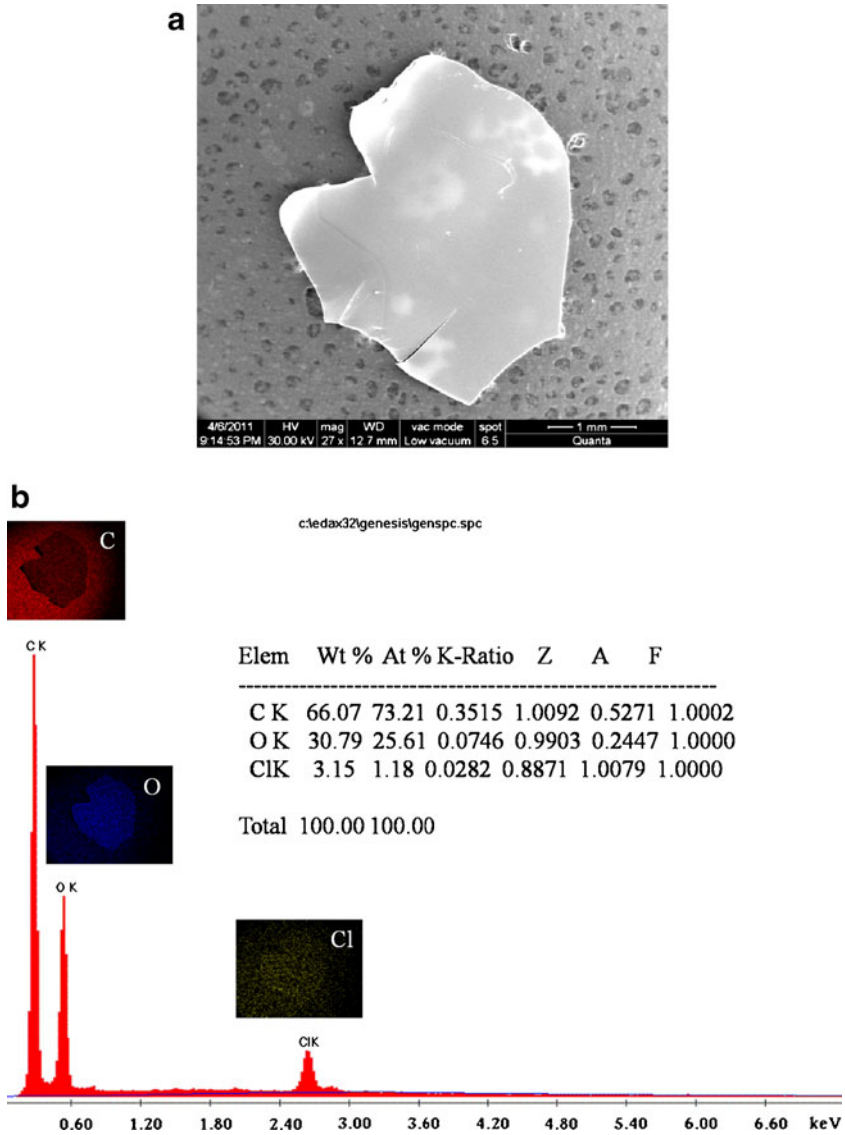


**Fig. 2** SEM image for Li $ClO_4$ included starch film (**a**) and EDAX spectra for Li-doped starch film (**b**). The *inset* inside **b** shows the elemental composition for carbon, oxygen, and chlorine in the film

*Raman spectroscopy* Figure 4b shows the Raman spectra for starch powder. Peaks were observed at 273, 355, 424, 482, 526, 603, 707, 781, 860, 923, 1,049, 1,100, 1,205, 1,263, 1,334, 1,388, and 1,458 $cm^{-1}$. Here strong peak at 482 and the neighboring weak peaks at 424 and 526 $cm^{-1}$ is attributed to skeletal modes (ring bending). Peak at 860 $cm^{-1}$ is associated with C–H deformation. Peak at 923, 1,049, 1,100, and 1,263 $cm^{-1}$ associated with C–O–H deformation. Peak at 1,205 $cm^{-1}$ is associated with $CH_2$ and C–O–H deformation. Peak at 1,334 $cm^{-1}$ is associated with C–O–H bending and $CH_2$ twist. Peak at 1,388 $cm^{-1}$ is due to C–H and C–O–H deformation. Peak at 1,458 $cm^{-1}$ is due to $CH_2$ symmetry deformation [22]. Figure 4c shows the Raman intensity of the starch films (one with 23% glycerol and another with 23% glycerol and 5% $LiClO_4$) along with the starch powder. It is observed that unlike starch powder, the films did not show any significantly tall peaks. Also, the intensities for the films were greater than that of the powder. This is attributed to the amorphous nature of the films. This is supported by the XRD data in Fig. 4a.

*FTIR spectroscopy* Figure 4d shows the FTIR spectra for starch films and its constituents. Infrared spectroscopy has been used for investigating changes in starch structure on a short-range molecular level. The original hydrogen bonds between starch molecules are destroyed by glycerol and make it thermoplastic. Various bands are present in starch. Peaks at 3,345 $cm^{-1}$ are assigned to OH stretching, 2 920 $cm^{-1}$ to CH stretching, 1 645 $cm^{-1}$ to OH bending, 1 530 $cm^{-1}$ to amide band, 1,450 $cm^{-1}$ to CH bending, 1,410 $cm^{-1}$ to OH bending, 1,330 $cm^{-1}$ to CH bending, 1,260–1,210 $cm^{-1}$ to OH bending, 1,200 $cm^{-1}$ to OH bending, 1,150 $cm^{-1}$ to CO stretching/OH bending,

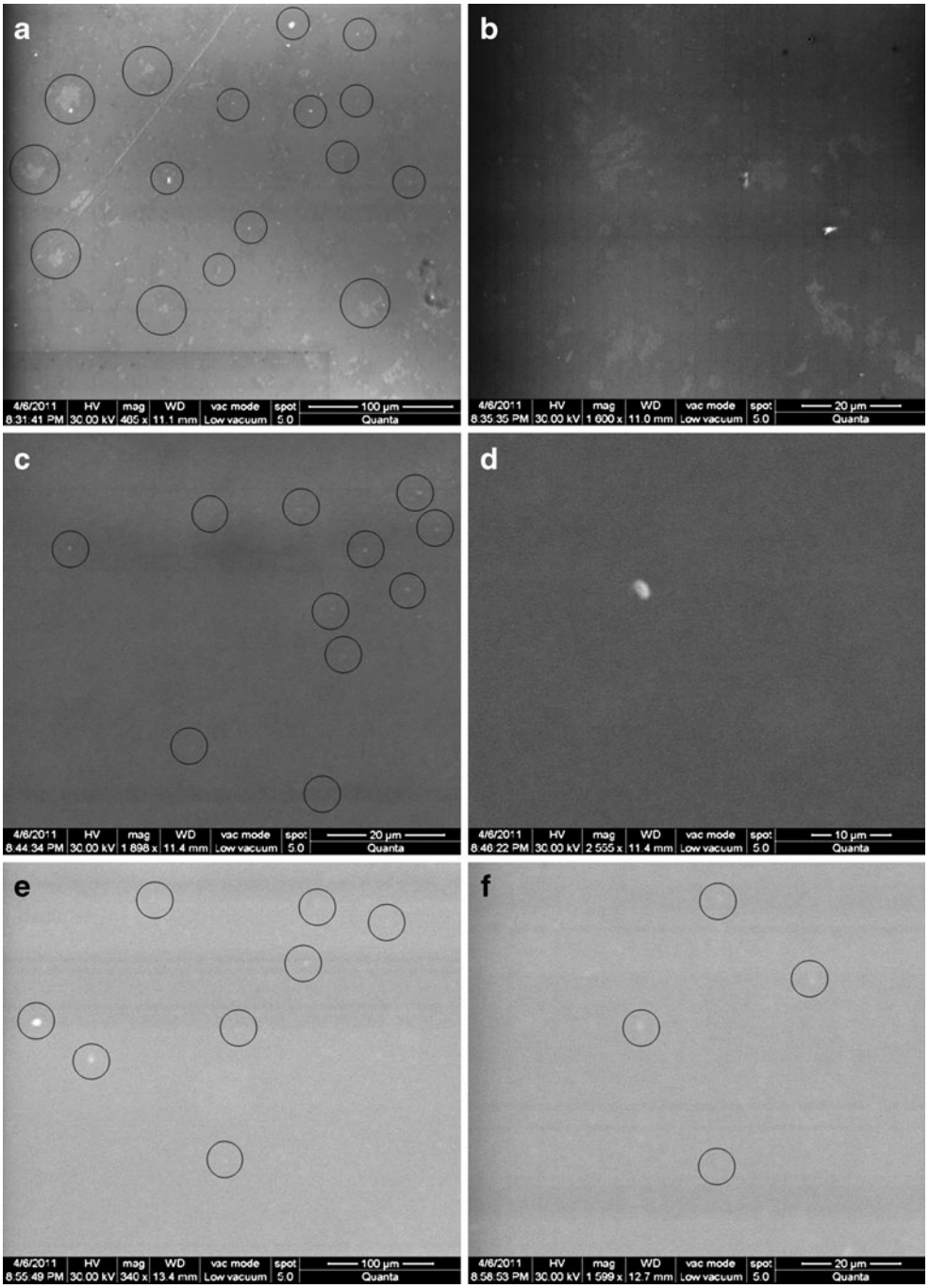


**Fig. 3** SEM images of **a**, **b** starch with 0% glycerol, **c**, **d** starch with 23% glycerol, and **e**, **f** starch with 23% glycerol and 5% $LiClO_4$

1,070 $cm^{-1}$ and 1,020 $cm^{-1}$ to CO/CC stretching and 940, 860, 750–700, and 600–520 $cm^{-1}$ to Pyranose ring vibrations [23]. The peak at 1,645 $cm^{-1}$ is due to water present in the starch. The bands at 1,047 and 1,022 $cm^{-1}$ are associated with the ordered and amorphous structures of starch, respectively [21]. The peak at 994 is sensitive to water content [24]. For glycerol, the broad absorption band associated with the hydroxyl groups of glycerol appears at 3,250 $cm^{-1}$ and the carbon–oxygen absorption characteristic occurs at 1,030 and 1,100 $cm^{-1}$, respectively [25].

It was observed that in the films containing glycerol, the broad band for starch at 3,345 $cm^{-1}$ (characteristic of OH stretching) seemed to increase in its height, indicating that the presence of glycerol would create more hydrogen bonds. This leads to an assembly of plasticizer molecules, leading to a greater increase in the hydroxyl group interactions and therefore having an increase in the height at the band at 3,345 $cm^{-1}$. The peak at 2,920 $cm^{-1}$ which is characteristic of H–C stretching became double peak for films containing glycerol. This is because the H–C

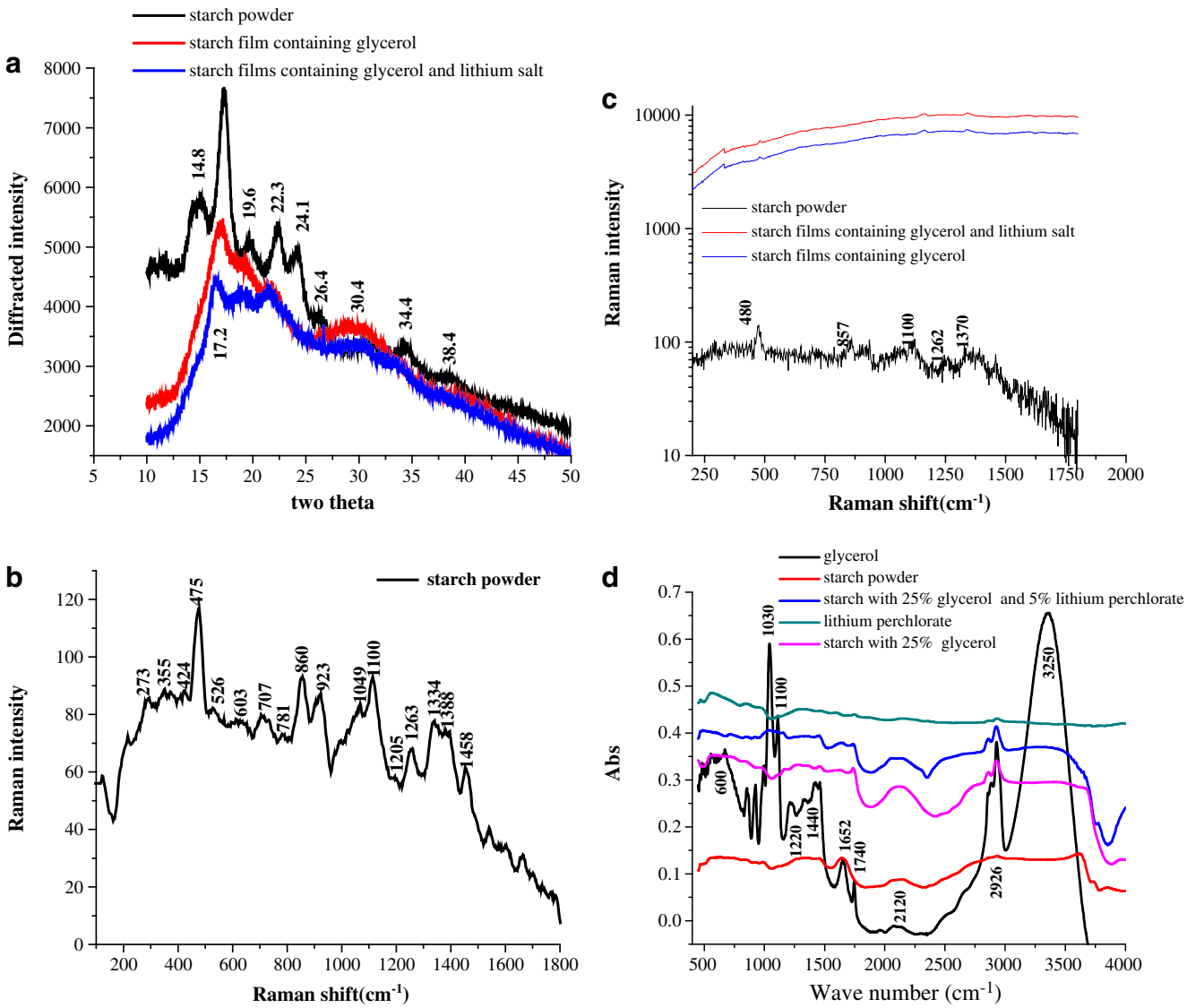


**Fig. 4** **a** XRD for the starch powder and starch films showing decrease in crystallinity with the formation of films. **b**, **c** Raman intensity for the starch powder and starch film. **d** FTIR for the starch films and its constituents

stretching for glycerol (2,926 $cm^{-1}$) is slightly different from that of starch (2,920 $cm^{-1}$). The peak at 2,120 $cm^{-1}$ is enhanced in the films containing glycerol. The peak at 1,645 for starch is due to water. It is observed that this peak also appears in the films, indicating the presence of trapped water. The peak at 1,741 $cm^{-1}$ appears in the films. It is not present in native starch but is present in glycerol. However, its height compared to its neighboring peak (1,645 $cm^{-1}$) is more in films than in native starch or glycerol. This indicates that though water is there in the films, its content is less. Starch films having glycerol seem to have their peaks at 1,106 $cm^{-1}$ as slightly more than that of native starch. This is more pronounced in the starch films containing $LiClO_4$ along with glycerol. Since carbon–oxygen absorption characteristic band occurs at 1,106 $cm^{-1}$, this implies that the inclusion of glycerol changes the microenvironment around the C–O groups. Lithium salt also showed some peaks at 2,926 and 1,330 $cm^{-1}$; the peaks were very short compared to that of glycerol and starch. Therefore, its influence in the spectral characteristics of the films is less.

## DSC

Two peaks were observed at~−85 and −30 °C (Fig. 5a). The peaks are not very prominent. This is because gelatinized starch has less crystallinity. However, when the spectra were analyzed using baseline correction (in origin), the peaks became clearer as shown in Fig. 5b. After analyzing, the peaks are observed at −85 and 30 °C. The presence of two separate peaks indicates that starch and glycerol are not

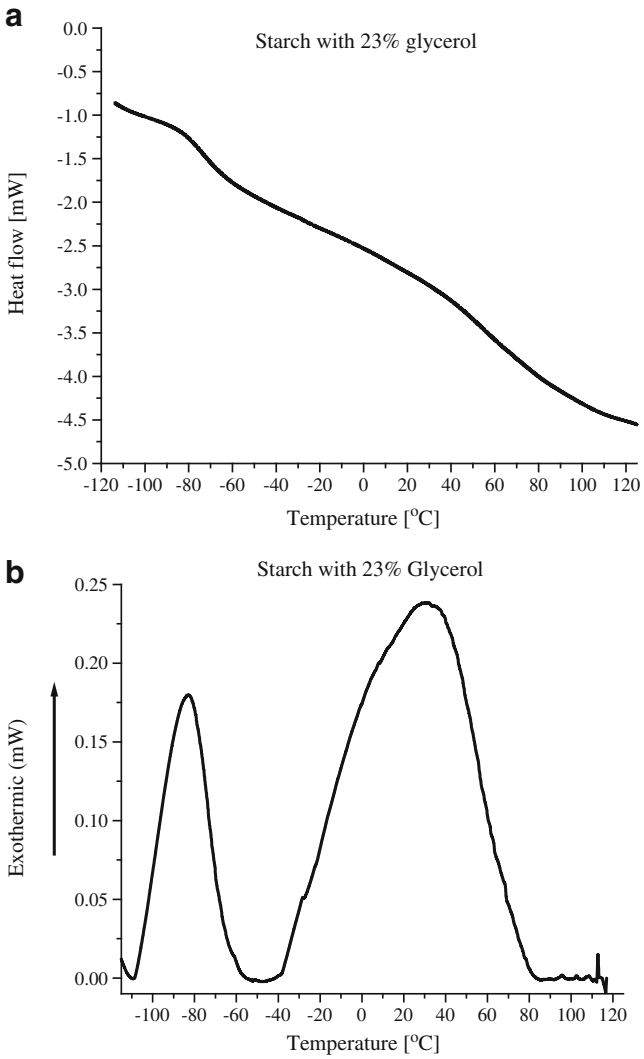


**Fig. 5** **a** DSC of starch with 23% glycerol showing peaks at −85 and 30 °C. **b** After flattening, the peaks clearly show distinct peaks

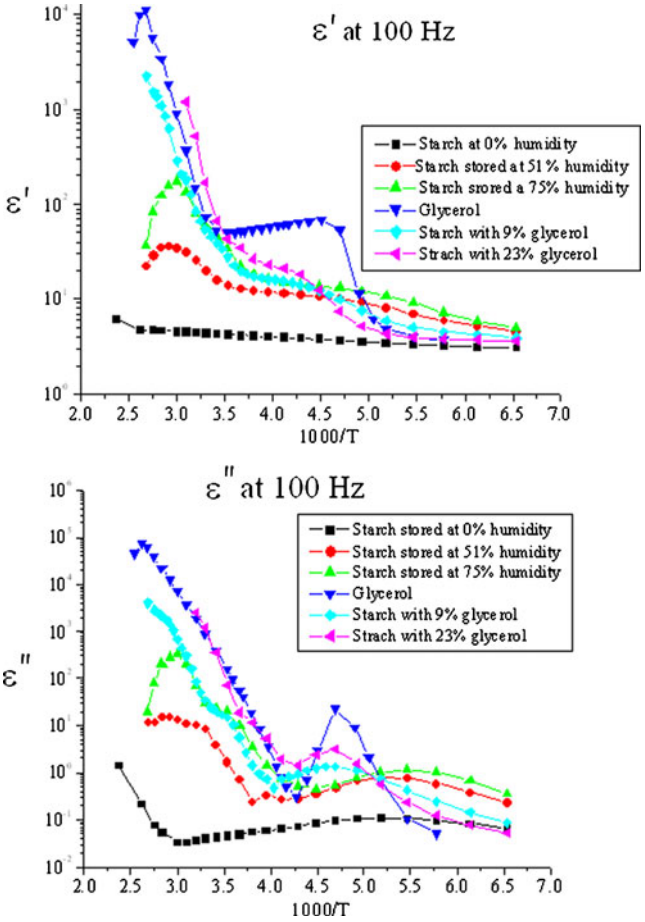


**Fig. 6** Dielectric constant and loss as a function of temperature at 100 Hz for starch samples

completely miscible. The $T_g$ for glycerol is −83 °C [26]. The $T_g$ for dry starch is 230 °C. The peak at −85 °C for starch with 23% glycerol is due to glycerol phase and the peak at 30 °C is due to starch–glycerol phase containing miscible starch and glycerol.

## Dielectric behavior

Some of the dielectric characteristics like tan $\delta$, relaxation times, and dielectric strengths are discussed as follows.

### *Dielectric constant and loss*

Figure 6 shows the variation of dielectric constant (real part) and dielectric loss at 100 Hz for the starch samples. It is observed from the dielectric loss spectra that the peaks for dry starch is broad and has maximum intensity at~−85 °C. The intensity of the peak for dry starch is lesser than that of all other samples. There is one relaxation observed in the case of dry starch at low temperatures, while at temperatures above 80 °C another relaxation is observed. For samples of starch with water in it, a relaxation is observed at low temperatures at positions close to that of dry starch. Another relaxation is observed in the temperature region (0–50 °C). For glycerol, a sharper peak (compared with other samples) is observed at~−60 °C. No relaxation is observed at higher temperatures. For starch with 9% and 23% glycerol, a peak is observed at the position same as that of glycerol (~−60 °C) and one more is observed at higher temperatures in the range (0–50 °C). The dependence of dielectric strength and dielectric loss upon temperature for 0.1 Hz, 1 Hz, 10 Hz, 100 Hz, 1 kHz and 10 kHz is supplied in the supporting information (Figs. S1–S6).

### *Tan delta*

Figure 7 shows the variation of tan $\delta$ at 10 Hz and 1 kHz for glycerol-plasticized starch films and starch films with varying water content (0%, 51%, and 75%, respectively).

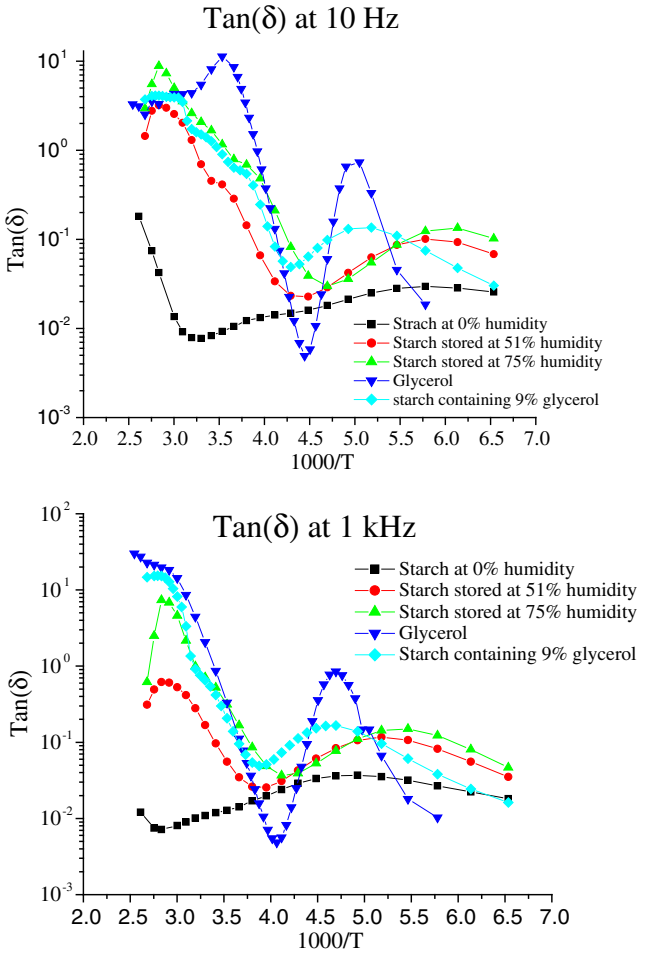


**Fig. 7** Tan delta plots for starch samples at 10 Hz and 1 kHz

*At 10 Hz* For dry starch, it was observed that there are peaks at ~ −100 and −10 °C. For starch samples in 51% RH and 75% RH, at 10 Hz the peaks were observed at −100 and – 10 °C, respectively, at the low temperature region. Additional peaks were observed at 10 °C (for 51% RH), −10 °C (for 75% RH), and ~ 80 °C for (51% RH and 75% RH). For glycerol, peaks were observed at −72 and 10 °C. For starch containing 9% glycerol, the peak at the low temperature region is at the same position as that of glycerol (−72 °C). For higher temperatures, it follows the same trend as in the starch samples in 75% RH.

*At 1 kHz* For dry starch, a peak was observed at~−70 ° C. For starch samples in 51% RH, peaks were observed at ~ −80 and 75 °C. For starch samples in 75% RH, the peaks were observed at ~ −85, 20, and 75 ° C. For glycerol, peaks were observed at −60 and ~ 80 °C. For starch with 9% glycerol, peaks were observed at ~ −60, 30, and 80 °C. For both frequencies, it was observed that the height of the peaks for dry starch is lesser than that for all other samples.

The difference in the peak position for starch with glycerol from that of dry starch or wet starch indicates that glycerol has a greater effect upon the DRS spectra at low temperature regions. Since starch and glycerol are not completely miscible, the effect of glycerol is bound to be greater due to the high polarity of glycerol.

*Relaxation times*

Figure 8a, b shows the variation of relaxation times as a function of temperature for the samples. The temperature range is split into two parts −132 to 0 °C (Fig. 8a) and from 0 to 180 °C (Fig. 8b) for clarity. For dry starch, it was observed that at low temperature regions (from −120 to −30 °C), the relaxation process obeys an Arrhenius behavior. Using the expression for Arrhenius behavior, $\tau=\tau_0 \exp(E_a / kT)$, the activation energy was found to be 41 kJ mol$^{-1}$. At higher temperatures, one more relaxation with activation energy of ~41 kJ mol$^{-1}$ was observed. For starch stored in 51% RH, it is observed that at low temperature regions

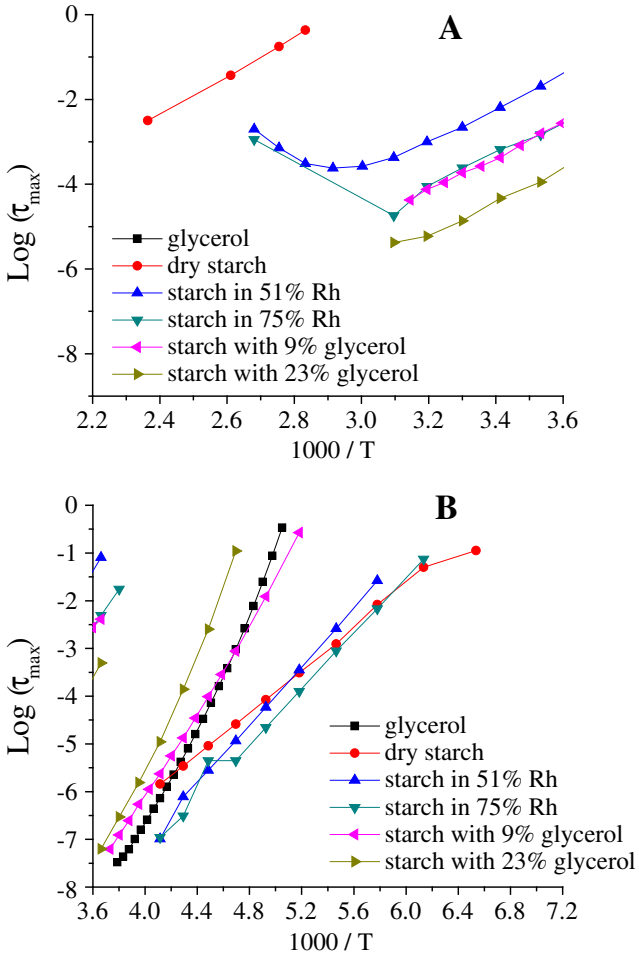


**Fig. 8** Relaxation times for starch samples as a function of temperature

(−100 to −30 °C) the relaxation obeys an Arrhenius behavior. The activation energy is 58.5 kJ mol$^{-1}$. This is in agreement with the results obtained by Tapas pal Majumder [12]. Another relaxation was observed from 0 to 50 °C with activation energy of ~75 kJ mol$^{-1}$. As the temperature is further increased (60–100 °C), the relaxation time increases. This could be attributed to the greater mobility of water molecules due to thermal effects. The activation energies for starch stored in 75% RH is nearly the same as that of starch stored in 51% RH. However the value of $\tau_{max}$ is greater in starch with 51% water than in starch stored in 75% starch both at low temperatures and at high temperatures. For starch stored in 75% RH, it is observed that at low temperature region (−110 to −30 °C) the relaxation obeys an Arrhenius behavior. The activation energy is 55 kJ/mol. At higher temperatures (from −10 to 50 °C), another relaxation was observed and it obeys the Arrhenius relationship with activation energy of 76 kJ mol$^{-1}$. The relatively low values of activation energies for dry starch (41 kJ mol$^{-1}$) and for wet starch (55 kJ mol$^{-1}$) at low temperatures indicate the presence of bound water and since it is Arrhenius it is a local relaxation process. The addition of water increases the space between the chains decreasing the sterical hindrance for the local chain motion and opens the fixing hydrogen bonds. The water dipoles adsorbed increases the effective dipolar moment of the polar sites. It is observed that for starch with 51% and 75% humidity, log ($\tau_{max}$) decreased with increasing temperatures and then increased after attaining a peak at~80 °C. This indicates the stiffening of the membranes due to evaporation of water. Vogel–Fulcher–Tammann (VFT) behavior was observed for segmental $\alpha$ relaxation at temperatures close to $T_g$. The VFT expression is $\tau_{max}=\tau_0 \exp(B/T-T_0)$ where $\tau_0$ and $B$ are constants. Glycerol was observed to obey a VFT behavior from −75 to −10 °C. No additional relaxations were observed at higher temperatures. For starch with glycerol (9% and 23%), VFT behavior was observed from −75 to −10 °C, and at higher temperatures (from 0 to 50 °C) Arrhenius behavior was observed. From 0 to 50 °C, for starch with 9% glycerol, the activation energy is 73 kJ mol$^{-1}$, and for starch with 23% glycerol the activation energy is 82 kJ mol$^{-1}$. For starch with glycerol samples at temperatures more than 50 °C, electrode polarization effect was observed, yielding high values for dielectric strength.

Since no relaxation was observed for dry starch at temperatures from 0 to 50 °C, the relaxations observed at temperatures from 0 to 50 °C in starch samples having glycerol should be due to water trapped in the starch films during film formations.

*Dielectric strength*

Figure 9 shows the dielectric strength of the starch samples as a function of temperature. The dielectric strength for dry

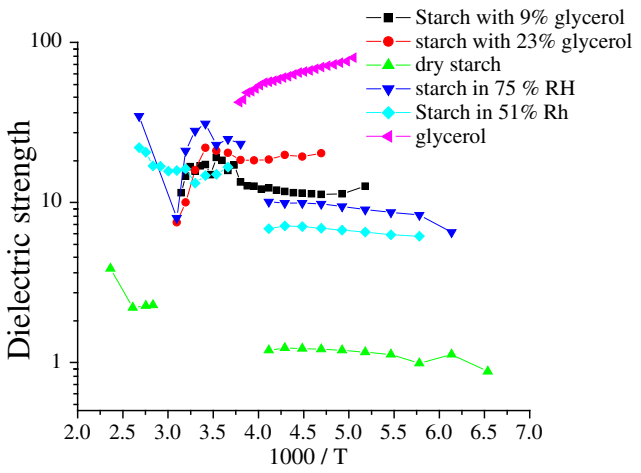


**Fig. 9** Dielectric strength for starch samples as a function of temperature

starch at low temperatures increases gradually from 0.9 to 1.1. Its low values indicate that it is local process. At temperatures from 80 to 150 °C, its value rises from 1.8 to 3.4. This also indicates that it is a local process and is associated with the stiffening of starch due to water molecules dissociating from it. For wet starch with 51% RH at temperatures from −100 to −30 °C, the dielectric strength increases gradually from 6.34 to 7.04, while for temperatures from 20 to 100 °C it increases from 14.18 to 19.18. This is indicative of Maxwell–Wagner–Sillars (MWS) relaxation. MWS relaxation arises from charge carriers accumulated at the interphase between amorphous and crystalline regions. For wet starch with 75% RH at temperatures from −110 to −30 °C, the dielectric strength gradually increases from 7.9 to 10.1, and for temperatures from 20 to 40 °C it increases from 21.4 to 28.8. This indicates that the relaxation observed for wet samples is MWS type. Hence, the presence of water contributes to charge accumulation between the amorphous and the crystalline regions.

For glycerol, the dielectric strength is found to decrease gradually with increasing temperatures. It decreases from 80.1 to 42.2 for temperature range of −75 to −9 °C. For starch containing 9% glycerol, at temperatures from −80 to −5 °C the dielectric strength increases from 10.8 to 13.8 and from 0 – 45 it decreases from 18.1 to 13.9. For starch with 23% glycerol, at temperatures from −60 to 0 °C the dielectric strength changes from 18.3 to 20.1 while for temperature from 10 to 50 °C it decreases from 21.8 to 8.84. The values of the dielectric strength for starch with glycerol are indicative of MWS relaxation. At temperatures above 50 °C, electrode polarization was observed.

Conductivity

Figure 10 shows the conductivity of starch samples with glycerol with and without $LiClO_4$. The conductivities follow

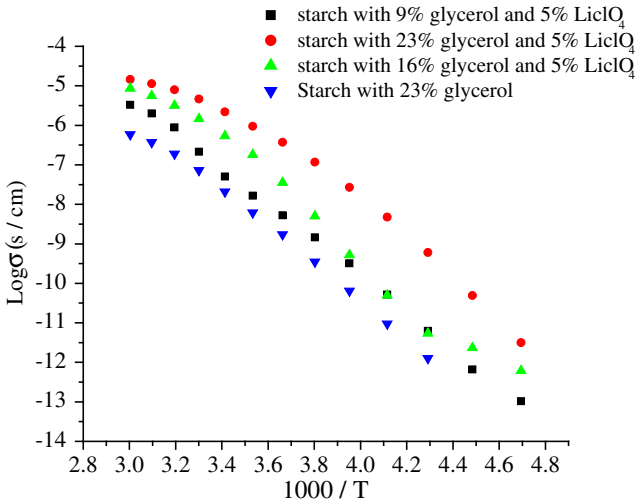


**Fig. 10** Conductivities of starch with glycerol as a function of temperature

a VFT distribution from −60 °C to 60 °C. In this temperature region, the dynamics of the polymer are described by VFT and therefore the conductivity follows the VFT behavior. At 20 °C, for dry starch, the DC conductivity is less than10 PS/cm, while the conductivities for starch stored at 51% and 75% RH are $2.06\times10^{-11}$ and $7.0\times10^{-10}$ S/cm. To the samples of starch with glycerol, 5% $LiClO_4$ was included while making the samples. It was observed that the conductivities at 20 °C of the samples having starch containing 9%, 16%, and 23% glycerol are $2.71\times10^{-10}$, $1\times10^{-9}$, and $3.61\times10^{-8}$ S/cm, respectively. It was observed that the conductivities at 20 °C of the samples having starch containing 9%, 16%, and 23% glycerol with 5% $LiClO_4$ were $5.06\times10^{-8}$, $5.36\times10^{-7}$, and $2.17\times10^{-6}$ S/cm, respectively. This indicates that there was a ~50× increase in conductivity for starch with 9% glycerol when 5%$LiClO_4$ was added to it and a ~165× increase in conductivity for starch with 23% glycerol when 5% $LiClO_4$ was added to it. As corn starch has branched and unbranched polymers leading to rich crystalline regions, it leads to compact and organized structures. Addition of glycerol to starch reduces the $T_g$ and may favor the movement of lithium ions and water, resulting in good ionic conductivity values.

### Model explaining the relaxation behaviors in starch films using dielectric measurements

Based on the dielectric measurements, the following model is proposed. The contribution to the dielectric spectra for dry starch is due to bound water at subzero temperatures. For higher water contents, contribution also comes due to the increased mobility of the polymer chains at intermediate temperatures (10 to 50 °C) due to the presence of water. At temperatures close to 100 °C, contribution to the dielectric spectra happens due to the stiffening of the matrix due to the evaporation of water. In films containing glycerol, there is only partial miscibility between starch and glycerol. Partial miscibility leads to greater contribution due to glycerol-rich phase to the dielectric spectra at low temperatures and greater contribution of water at higher temperatures to dielectric spectra. There is an increase in the conductivity with increasing glycerol concentrations in starch samples to which 5% $LiClO_4$ was included. The various components making the starch film is shown as a cartoon in Fig. 11.

## Conclusions

In this article, a detailed analysis of the dynamics of the polymers in starch films using dielectric spectroscopy has been presented. SEM images showed that starch and glycerol were not completely miscible. XRD and Raman measurements showed that the starch films were amorphous. FTIR spectra showed that the presence of glycerol in the films affected the local environment of the starch molecules. DSC results show that, in glycerol-plasticized starch films, starch and glycerol are not completely miscible. Two separate peaks, one at −83 °C (glycerol phase) and another at 30 °C (starch–glycerol) phase, were observed in DSC experiments with starch films containing 23% glycerol. Dielectric measurements showed that dry starch (starch with 0% humidity) has local relaxation at low temperatures (−120 to −30 °C) with an activation energy of 41 kJ $mol^{-1}$ indicating bound water and a relaxation at temperatures close to 100 °C indicating the stiffening of the relaxations as water dissociates from the starch. Addition of water showed two relaxations (both Arrhenius type), one at low temperatures and another at temperatures from 0 to

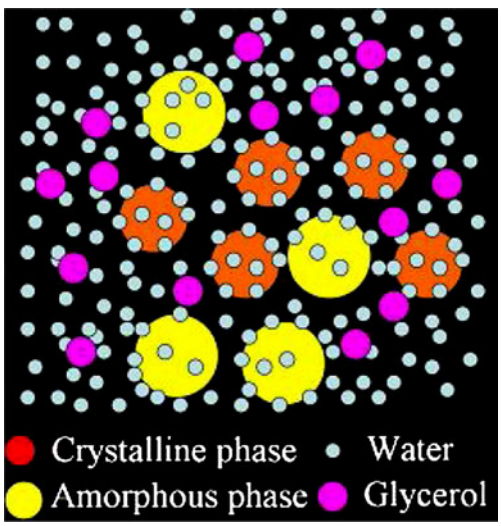


**Fig. 11** Various components of starch films

50 °C. For starch with glycerol, it was observed that $T_g$ was greatly reduced, leading to a VFT behavior at low temperatures (−60 to 0 °C). It was further observed that the DRS spectra were dominated by the presence of glycerol at low temperatures. The high influence of glycerol upon the dielectric spectra at low temperatures could be because of the high polarity of glycerol-rich phases in the starch films (due to being not completely miscible of starch and glycerol) when compared to that of starch or water bound to starch. At higher temperatures (0–50 °C) in starch containing 9% and 23% glycerol, the spectra were influenced by the presence of water trapped in the formation of the films. The position of peaks from useful dielectric parameters like tan $\delta$, $\varepsilon'$, and $\varepsilon''$ confirms that the influence of glycerol upon the dielectric spectra is greater at low temperatures while that of water is greater at higher temperatures. It was observed that, for starch films containing glycerol, the dielectric spectra at low temperatures (−100 to −30 °C) were highly influenced by the presence of glycerol. At higher temperatures (0–50 °C), the spectra were influenced by the presence of water in the films. The result is explained using a model based on the immiscibility of starch and glycerol.

**Acknowledgment** The author would like to gratefully thank Prof. James Runt of Department of Materials Science and Engineering, The Pennsylvania State University, USA, for providing the opportunity to begin this research as a postdoctoral researcher in his laboratory. The author also gratefully thanks Dr. Georgios Polizos of Oak Ridge National Lab, USA, for his valuable help in dielectric measurements. The author gratefully thanks Prof. T. Pradeep of DST unit of Nanoscience, Department of Chemistry and Sophisticated Analytical Instrument Facility, Indian Institute of Technology Madras, India, for providing the facility for imaging with SEM. Help due to Mr. Udaya Sankar of DST unit of Nanoscience, Department of Chemistry and Sophisticated Analytical Instrument Facility, Indian Institute of Technology Madras, India, in SEM imaging is also much appreciated. The author gratefully thanks Prof. S. Moorthy Babu of Crystal Growth Center of Anna University, Chennai, India, for providing the facility to make Raman spectroscopy measurements. Part of the project was carried out with the research grant "Research Support Scheme for Young Faculty of Anna University" received by the author from the Center for Technology Development and Transfer of Anna University—Chennai in the year 2010.

## References

1. Viera DF, Avellaneda CO, Pawlicka A (2008) Mol Cryst Liq Cryst 485:95
2. Pawlicka A, Sabadini AC, Raphael E, Dragunski DC (2008) Mol Cryst Liq Cryst 485:56
3. Banks W, Greenwood CT (1975) Starch and its components. Edinburgh University Press, Edinburgh
4. Phillips PJ (1994) In: Hurle DTJ (ed) Handbook of crystal growth 2. Bulk crystal growth. Part B: growth mechanisms and dynamics. North-Holland, New York, p 1167
5. Cameron RE, Donald AM (1993) J Polymer Sci, Part B: Polymer Phys 31:1197
6. Einfiled J, Meiβner D, Kwasniewski A (2001) Prog Polym Sci 26:1419
7. Orford PD, Parker R, Ring SG, Smith AC (1989) Int J Biol Macromol 11:91
8. Viciosa MT, Dionisio M, Silva RM, Reis RL, Mano JF (2004) Biomacromolecules 5:2073
9. Eineldt J, Meiβner D, Kwasniewski A (2000) Macromol Chem Phys 201:1969
10. Eineldt J, Meiβner D, Kwasniewski A (2003) J Non-Cryst Solids 320:40
11. Eineldt J, Meiβner D, Kwasniewski A, Eineldt L (2001) Polymer 42:7049
12. Majumder TP, Meiβner D, Schick C (2004) Carbohydr Polym 56:361
13. Butler MF, Cameron RE (2000) Polymer 41:2249
14. Shogren RL (1992) Carbohydr Polym 19:83
15. Forsell PM, Mikkila JM, Moates GK, Parker R (1997) Carbohydr Polym 34:275
16. Lourdin D, Bizot H, Colonna P (1997) Macromol Symp 11:179
17. Lourdin D, Coignard L, Bizot H, Colonna P (1997) Polymer 38:5401
18. Lourdin D, Ring SG, Colonna P (1998) Carbohydr Res 306:551
19. Moates GK, Noel TR, Parker R, Ring SG (2001) Carbohydr Polym 44:247
20. Wubbenhorst M, Turnhout JV (2002) J Non-Cryst Solids 305:40
21. Sevenou O, Hill SE, Farhat IA, Mitchell JR (2002) Int J Biol Macromol 31:79–85
22. Cael JJ, Koenig JL, Blackwell J (1975) Biopolymers 14:1885–1903
23. Delval F, Crini G, Bertini S, Morin-Crini N, Badot P-M, Vebrel J, Torri G (2004) J Appl Polym Sci 93:2650–2663
24. van Soest JJG, Tournois H, de Wit D, Vliegenthart JFG (1995) Carbohydr Res 279:201–204
25. Holser RA (2008) J Appl Polym Sci 110:1498–1501
26. Ryabov YaE, Hayashi Y, Gutina A, Feldman Y (2003) Phys Rev B 67:132202